Reliability Analysis for Components under Thermal Mechanical Loadings

Julio Pulido, PhD, Reliasoft Corporation

Key Words: Accelerated Life Test, Thermal Mechanical Stress, Structural Testing, Reliability Deterioration, Acceleration Factors

SUMMARY & CONCLUSIONS

Environmental and Operational Stress Testing is the most common approach to precipitating structure latent defects before the manufacturing of products. This testing consists of applying environmentally induced stresses to the product. Typically, these environmental stresses for mechanical structural automotive components consist of vibration loading based on road input and/or self-induced vibration with cycling temperatures between a high and low extreme.

Many components in most fields of engineering are subjected to fatigue at elevated temperatures. High – temperature fatigue is mainly a concern at temperatures above 30 or 40 percent of the absolute melting temperature. Since some of these components are costly and safety-critical, it is understandable that there is a significant interest in proper characterization of fatigue behavior at high temperatures.

On most cases strain life characteristic is not known for a given application and or a given material. To further complicate the component application can be in an environment where more than one failure mode due to the application type can be observed.

This paper presents a practical testing methodology used to determine product's operational life given high temperature operational application and results are compared with field observations.

1.0 THE APPLICATION

Reliable life assessment of structural components using the state-of-the-art life prediction models forms the basis of good design and of design modifications which may lead to component life extension in product applications like heaters, resistors or heat transfer coils.

Hot section components are designed to operate in high temperature environments with high thermal gradients. They are subject to cyclic strains that are induced thermally as well as mechanically. Under these cyclic temperatures and strains, thermo-mechanical fatigue (TMF) damage occurs in the material, leading to initiation of cracking and subsequent crack growth.

The system under evaluation is a resistor used for energy dissipation (Figure 1). The resistor material is a steel based alloy. During braking, the motor fields are connected across either the main traction generator (diesel-electric locomotive or large trucks) or the supply (electric locomotive) and the motor armatures are connected across either the brake grids or supply line. The system's rolling wheels turn the motor armatures, and if the motor fields are now excited, the motors will act as generators.

For a given direction of rotation, current flowing through the motor armatures during braking will be opposite to that during motoring. Therefore, the motor exerts torque in a direction that is opposite from the rolling direction. Braking effort is proportional to the product of the magnetic strength of the field windings, times that of the armature windings.

For permanent magnet motors, dynamic braking is easily achieved by shorting the motor terminals, thus bringing the motor to a fast abrupt stop. This method, however, dissipates all the energy as heat in the motor itself, and so cannot be used in anything other than low-power intermittent applications due to cooling limitations.

During repeated startups, the resistor components experience cyclic strains, which are induced both thermally by rapid temperature changes, and mechanically by product application forces (vibration, impact). The design uses steel as heating material when high voltage is applied to the system due to dynamic braking of the system.

Figure 1 Resistor/ Heater

At the microstructural level, damage processes occurring under TMF are more complex than under isothermal fatigue. A complex interaction between thermally activated, time-dependent processes is involved. These include creep/relaxation, and metallurgical aspects acting jointly with mechanical fatigue mechanisms (See Figure 2). Factors such as frequency, wave shape, and creep/ relaxation, which are secondary at room temperature environments, have appreciable importance at high temperature.

Components that operate at elevated temperatures are often subjected to transient temperature gradients due to start-up and shut-down. During the start-up and shut-down cycle, thermally induced cyclic stresses can occur. Components subjected to this behavior often operate at temperatures such that both fatigue and creep damage occurs and each must be taken into account.

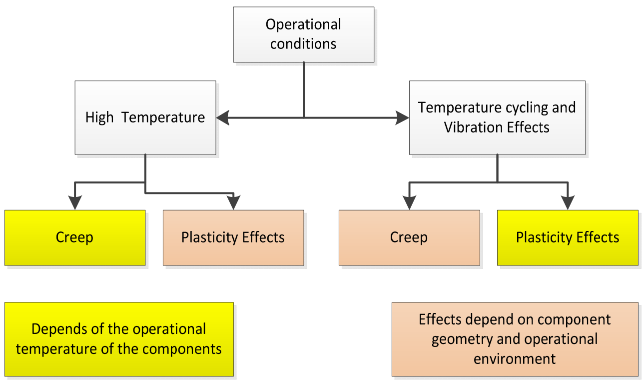

Figure 2 Operational Conditions Identified and associated effects

Sophisticated life prediction models have been developed to take creep-fatigue interactions and other damage effects into account, and so improve life predictions under TMF conditions.

During the literature survey, it was found that there are numerous modeling techniques available for thermo fatigue based on experiments using smooth specimens. For TMF crack initiation, more than one hundred life prediction approaches and variations exist [1] but they are dependent upon loading and material type.

3.0 THERMAL MECHANICAL FATIGUE

Thermal-Mechanical fatigue is the synergistic damage process caused by cyclic thermal and mechanical loading, and the theory of TMF addresses the creep-fatigue interactions that occur. When hot-section components are subject to high temperature thermal cycles concurrently with mechanical strain cycles, TMF conditions resulting in microstructural damage occur. The lifetime of the components under such TMF loading is found to be quite different from that obtained in isothermal low-cycle fatigue tests conducted at the maximum temperature of operation, where creep damage of the material would be greatest.

When both thermal and mechanical cycles vary in an arbitrary manner, predicting lives becomes very difficult. Modern laboratory testing techniques allow realistic simulation of cycle shapes representing actual service conditions. There are two extreme modes; in-phase and out-of-phase cycles, as shown in Figure 3. Under in phase cyclic loading conditions, the maximum tensile strain occurs at the same time as the peak temperature, and the maximum compressive strain occurs at the minimum temperature. In contrast, under out-of-phase cycles, the maximum tensile strain occurs at the minimum temperature, and maximum compressive strain at the peak temperature.

A single damage mechanism is not adequate for characterizing all TMF damage, therefore a number of damage mechanisms and damage models have been proposed. For this issue the approach taken was to consider creep and thermal fatigue effects based on the temperature of the material.

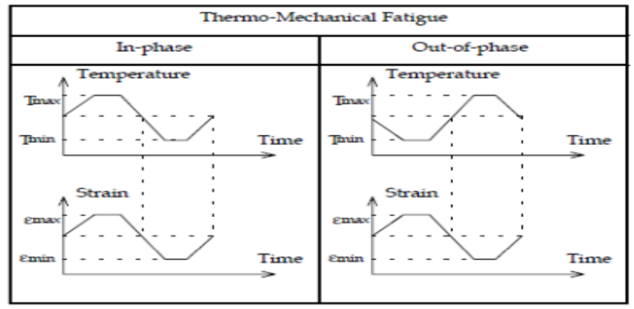

Figure 3 In-phase and Out-of-phase TMF loading patterns

The more sophisticated models require many variables and associated parameters to represent the principal damage mechanisms in the life equations. The variables include elastic, inelastic, and total strain-ranges, dissipated strain energy, temperature, frequency, hold time, strain rate, and mean stress [2].

4.0 LIFE PREDICTION METHODOLOGIES

Thermal-Mechanical fatigue life prediction models take into account the interaction between fatigue and creep at varying temperatures. The difficulty in understanding and predicting the interaction behavior has stimulated significant research effort in finding good life prediction models. The models used include damage-based criteria, stress-based criteria, strain-based criteria and energy-based criteria.

The following review focuses on the more popular and advanced TMF models, comprising the Damage Summation (DS), Frequency Separation (FS), and Total Strain Version of SRP (TS-SRP).

4.1 Damage Summation Model

The linear Damage Summation (DS) model (also called the linear life fraction or linear cumulative damage) is the simplest expression for creep-fatigue life prediction. It ignores the microstructural details of the damage process. It is defined as follows [3]:

$$D_{fatigue} + D_{creep} = D_{total} \tag{1}$$

D_{total} is the total damage, $D_{fatigue}$ and D_{creep} are the fatigue damage and creep damage respectively. The damage summation rule assumes that failure occurs when the sum of the fatigue damage and the creep damage is equal to a critical value. By means of the Miner rule [4] for fatigue damage and Robinson rule [5] for creep damage, with repeated application of a single simple cycle, Equation (1) becomes:

$$N_f = \left(\frac{1}{N_p} + \frac{\tau}{T_c} \right) \quad (2)$$

N_f is the number of cycles to failure at a given strain-range, and N_p is the pure fatigue life at that strain-range. The creep damage fraction in each cycle is τ/T_c in which τ is the hold time at a given stress in a cycle and T_c is the time to rupture under static creep at that stress.

Under thermal-mechanical strain cycles, the creep damage consists both of a loading creep strain (as load/temperature is held constant or increases with time above a threshold creep value) and dwell creep strain (when strain is held constant over the hold time resulting in stress relaxation). Ellison [6] modified life prediction by this fraction rule to deal with the changing strain, summing over τ/T_c (approximated as a series of steps) as follows:

$$(\frac{\tau}{T_c})_{total} = \sum(\frac{\tau_i}{T_{ci}})_{loading} + \sum(\frac{\tau_i}{T_{ci}})_{dwell} \quad (3)$$

Analogously to summing the creep damage fraction, fatigue damage is obtained by summing the cyclic damage under differing loadings. The linear damage summation in Equation (2) should then be written as:

$$\sum\frac{N_i}{N_{pi}} + \sum\frac{\tau_i}{T_{ci}} = D_{total} \quad (4)$$

Where the subscript i refers to specific fatigue conditions. In many cases, the DS model can adequately predict experimental behavior for engineering applications, especially for thermal fatigue [7].

4.2 Frequency Separation Model

The frequency separation (FS) model incorporates the effect of cyclic frequency upon the creep fatigue life. Coffin [8] extended the Coffin-Manson Law and postulated a power-law life relationship given in Equation (5) with three principal variables, inelastic strain-range $\Delta\varepsilon_{in}$, tension-going pseudo-frequency ϑ_t, and cycle-time unbalance ϑ_c/ϑ_t. ϑ_t and ϑ_c are reciprocals of the tension-going and compression-going times τ_t and τ_c respectively, as shown in Figure 4.

$$N_f = C\,\Delta\varepsilon_{in}^{\beta}\,\vartheta_t^m\,(\frac{\vartheta_c}{\vartheta_t})^k \quad (5)$$

C, β, m, and k are constants dependent on material, environment and temperature. They are determined by 'slow-fast' or 'fast-slow' tests. The FS model was developed to deal properly with very complex wave shapes. The concept of tension-going damage is based on the micro crack propagation process, assuming that low-cycle fatigue damage can be measured by the micro crack growth. During the tension-going part of the cycle the micro crack opens and advances while during compression the crack closes and does not advance. This simple modification separating tension-going and compression-going damage provided a significant error reduction in high temperature low-cycle fatigue life prediction.

In developing the FS model, Coffin [8] obtained good agreement between fatigue life predicted from the model and actual measured life in experiments using 316 stainless steel.

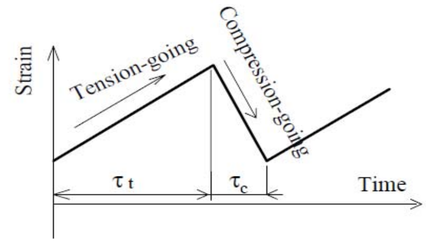

Figure 4 Slow-fast waveform cycles

4.3 Total Strain Version of Strain-Range Partitioning

For high temperature low-cycle, fatigue the failure process is affected by the time-dependent cyclic stress-strain behavior over the entire temperature range. To account for the time dependent portions of the cycle, Mason [ ] developed the strain-range partitioning method (SRP). The SRP life prediction model partitions the inelastic strain-range into time-dependent plasticity and time-dependent creep. Under cyclic reversed loading, there are four possible combination cycles of inelastic strain. The cycles types are: tensile plasticity reversed by compressive plasticity (PP), tensile creep reversed by compressive creep (CC), tensile creep reversed by compressive plasticity (CP) and tensile plasticity reversed by compressive creep (PC).

The model is based on the damage rule [15]:

$$\frac{1}{N_f} = \frac{1}{N_{pp}} + \frac{1}{N_{cc}} + \frac{1}{N_{cp}} + \frac{1}{N_{pc}} \quad (6)$$

In total strain version of the strain-range partitioning (TS-SRP), the various elastic strain versus life relations are assumed to follow a power law, parallel to the corresponding PP elastic life line on a log-log plot. Similarly it is assumed that on a log-log plot the various inelastic strain range versus life relations are parallel to the PP inelastic line. Hence the failure behavior is given by:

$$\Delta\varepsilon_{el} = B(N_f)^b \quad (7)$$

$$\Delta\varepsilon_{in} = C'(N_f)^c \quad (8)$$

and it can be shown that for the modified SRP Equations, (6) (7)-(8) that:

$$C' = \left[\sum F_{ij}\left(A_{ij}\right)^{1/c}\right]^c \quad (9)$$

F_{ij} are the strain-range fractions associated with PP, PC, CP and CC, and the coefficients A_{ij} are material constants determined experimentally. From the parallelism assumption (shown in Fig. 4), b and c are constants independent of cycle time and wave shape. B is the intercept of the elastic strain-range versus life relation, and C' is the intercept of the equivalent inelastic line for combined creep-fatigue cycles. Both B and C' are cycle time and wave shape dependent.

The total strain-range is the sum of the elastic strain-range and the inelastic strain range, so the total strain-range versus life equation can then be obtained as the following:

$$\Delta\varepsilon_T = \Delta\varepsilon_{el} + \Delta\varepsilon_{in} = B\left(N_f\right)^b + C'\,(N_f)^c \quad (10)$$

To apply this TS-SRP life prediction model the constants b, c, B and C' in Equation (10) must be determined. Flow behavior (i.e. the cyclic stress-strain curve which is the locus of reversal points of stabilized hysteresis loops) offers an additional means of gaining data for TS-SRP. By eliminating Nf from Equations (7) and (8), a relation between elastic and inelastic strain-ranges can be derived:

$$\Delta\varepsilon_{el} = B\,\left(\frac{\Delta\varepsilon_{in}}{C'}\right)^{b/c} \qquad (11)$$

This can be compared with a flow law (determined by experiment or by constitutive modeling):

$$\Delta\varepsilon_{el} = \Delta\sigma/E \; = K\,(\Delta\varepsilon_{in})^{n} \qquad (12)$$

Δσ is the stress range, E is Young's modulus, n is the cyclic strain-hardening exponent and K is the corresponding hardening coefficient. Equating the failure behavior in Equation (11) and the flow behavior in Equation (12) gives:

$$n = {}^{b}/_{c} \qquad (13)$$

$$B = K\,(C')^{n} \qquad (14)$$

The constants b and c are normally determined from PP failure tests, conducted in the high strain-range regime so that test times can be reduced and costs minimized. But obtaining an accurate value for b is difficult so that n may not exactly equal b/c. Thus, for better substantiation of n additional PP flow tests can be conducted when the specimen is cycled for long enough for material shakedown [9].

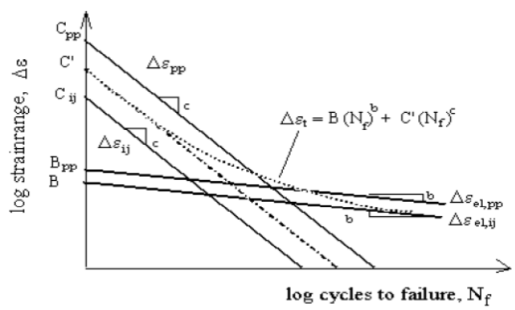

Figure 5 Strain-life relations for TS-SRP

5.0 TEST DESIGN

The following is the methodology for failure testing, since a constitutive model was not available to the engineering team assessing the product life.

The components are subjected to a variety of temperature, strain and load histories in service. These histories may produce material damage that could lead to component failure due to plasticity or creep as identified in the literature research.

When considering the wide range of operational conditions 700C to ambient (20°C to -40°C). For high temperature (T > 400°C) strong strain rate dependence exist on the yield stress of the material. Therefore testing should consider for effects above and below the 400°C. This behavior is characteristic of a creep mechanism. For lower temperatures, the material exhibits relative strain rate insensitivity which is characteristic of the plasticity deformation mechanism.

The above behavior was demonstrated by generating a series of isothermal constant strain rate experiments generating strain rate versus yield stress measurements for steel ASTM-1070 [10] Figure 6.

Therefore the Elastic modulus of elasticity will change at 400°C temperature.

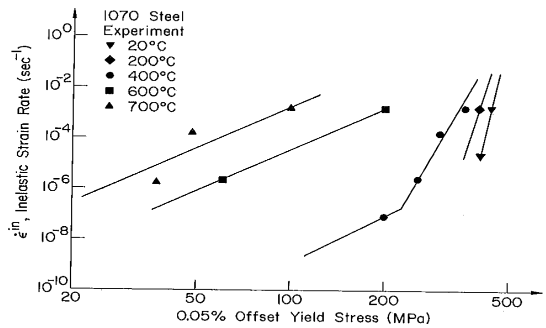

Figure 6 Failure mechanism behaviors

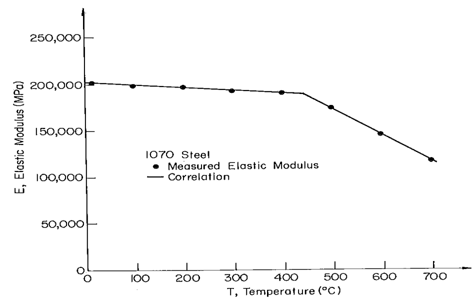

Figure 7 Elastic Modulus as function of temperature.

Figure 7 shows the high slope in the plasticity mechanism regime that corresponds to rate insensitive material behavior (T < 400°C) The lower slope of the power law creep deformation mechanism corresponds to rate sensitive material behavior (T > 400°C).

Based on the above information a test methodology oriented to high temperature (T > 400°C) was selected and the ramping strain was simulated by keeping the resistor energy rate of change similar to the application's maximum [11].

For the temperature cycling a temperature range that represents 95% of the population was selected. The total range is based on operational profiles generated using input from the sales and service groups.

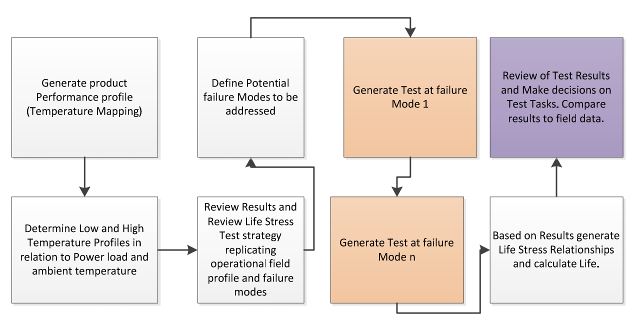

Figure 8 Test procedure

6. 0 TEST SET UP

A fixture was designed and a test was conducted for vibration, and temperature cycling (See Figure 8). Calibration of the head expander was performed before the fixture with the unit under test installed on the head expander. Center of gravity (COG) measurement and system balance was performed on the head expander with the device under test (DUT). Three sensors were used for location of the balance weights. This is critical in order to assure second order effects are not introduced in the system. The location of temperature sensors were based on thermal image of the unit since no Finite Element Analysis (FEA) was performed on the unit.

6.1 Sweep Test and Modal Test

Sweep and Modal Tests were conducted to find the resonance frequencies, with the input of 0.3g level acceleration in Y axis (vertical), swept from 5 to 50Hz with a 0.1Hz/s frequency sweep rate to confirm we had not resonance issues in the field and the vibration loading will not induce resonance.

6.2 Thermal Cycling Test

Acceleration factors were determined by comparing material property and measured stresses for actual user profiles against the stress levels evaluated during testing. Since no FEA was generated the factors will be defined based on the stress temperature and the operational temperature.

During testing, the unit under test was submitted to a vibration profile simulating the vibration and impact loading in the unit. Careful inspection of the structure was performed at every hour until a failure was observed. At that moment the time was recorded along with the failure mode. The vibration profile is not presented in this paper.

7.0 LIFE PREDICTION EVALUATIONS

7.1 Thermo Cycling with Vibration Loading

The results showed in Figure 9 indicated that the shape parameters of the Weibull distribution where very close for effect observed at high temperature level (963°K, 890°K) and lower operational levels (640°K, 550°K).

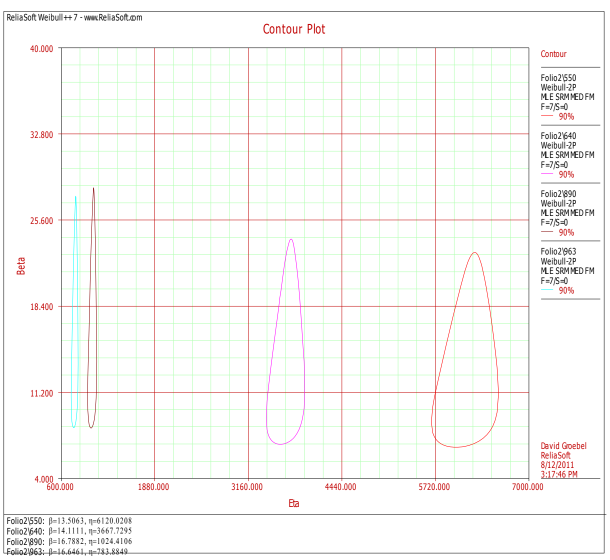

Figure 9 Contour Plots for Test Data

The failures observed at the higher levels were creep based as expected, but the ones at lower levels were a mixture of creep effects and plasticity. Since the shape factors are high and very close to each other the analysis was performed by combining the effects into one function.

The life analysis was performed for the highest temperature application in the field (790°K) showing a shorter life when compared with lower operational temperatures (400°K).

The results shown in Figure 10 and Figure 11 confirm the level of magnitude of the warranty data for the field applications at 790°K and 400°K operational temperature levels.

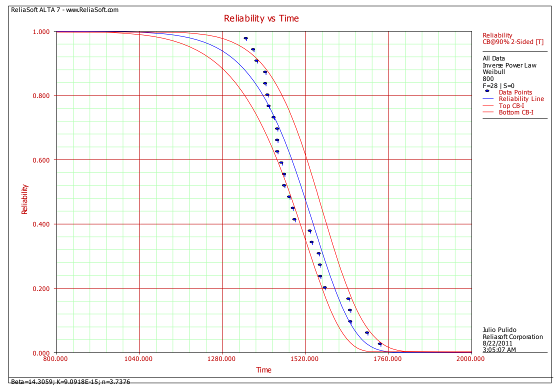

Figure 10 Reliability Function for 790°K

The results show correlation to current product performance in the field at higher operational temperatures but more testing is need to evaluate the components at lower temperature in order to determine the shape factors and the failure modes correlate to plasticity effects since the shape factors are too close for the current temperature levels tested.

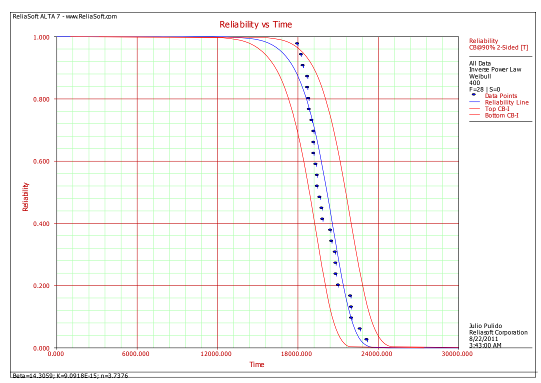

Figure 11 – Reliability Function for 400°K

REFERENCES

1. Halford, G., "Brief Summary of the Evolution of High-Temperature Creep-Fatigue Life Prediction Models for Crack Initiation," NASA-CP-3230, 1993.
2. Chaboche, J., "Lifetime Predictions and Cumulative Damage under High- Temperature Conditions," Low-Cycle Fatigue and Life Prediction, ASTM STP 770, C. Amzallag, B. N. Leis and P. Rabbe, Eds., American Society for Testing and Materials, pp. 81-104, 1982.
3. Taira, S., "Lifetime of Structures Subjected to Varying

Load and Temperature," Creep in Structures, N., J., Hoff (ed.), SPRINGER-VERLAG, pp. 96-124, 1962.
4. Miner, M., "Cumulative Damage in Fatigue," J. Applied Mechanics. Trans. ASME, 1952.
5. Robinson, E., "Effect of Temperature Variation on the Long-Time Rupture Strength of Steels," Transactions, ASME, Vol. 74, No. 5, pp. 777-780, 1952.
6. Ellison, E. and Zamily, A., "Fracture and Life Prediction Under Thermal- Mechanical Strain Cycling," Fatigue Fract. Engng Mater. Struct. Vol. 17, No. 1, pp. 53-67, 1994.
7. Spera, D., "Comparison of Experimental and Theoretical Thermal Fatigue Lives for Five Nickel-Base Alloys," Fatigue at Elevated Temperatures, ASTM STP 520, American Society for Testing and Materials, pp. 648-657, 1972.
8. Coffin, L. Jr., "The Concept of Frequency Separation in Life Prediction for Time- Dependent Fatigue," in 1976 ASME-MPC Symposium on Creep-Fatigue Interaction, MPC-3, American Society for Mechanical Engineers, New York, pp. 349-364, 1976
9. Saltsman, J. and Halford, G., "Procedures for Characterising an Alloy and Predicting Cyclic Life With the Total Strain Version of Strainrange Partitioning (SRP)," NASA TM - 4102, 1989
10. Sehitoglu, H and Slavik, D., "Constitutive Model for High temperature Loading – Part II", Pressure Vessels and Piping conference, 1987
11. Sehitoglu, H and Slavik, D., "Constitutive Model for High temperature Loading – Part I", Pressure Vessels and Piping conference, 1987
12. R.Stephens, A. Fatemi, R. Stephens and H. Fuchs, "Metal Fatigue in Engineering", John Wiley & Sons, 2001
13. American Society of Civil Engineers (ASCE), Committee on Fatigue and Fracture Reliability, "Fatigue and Fracture Reliability: A state-of-the-art Review", Journal of the Structural Division of American Society of Civil Engineers, vol. 108, 1982, pp 3-104
14. H. Chan and P. Englert, Accelerated Stress Testing Handbook, IEEE Press, 2001
15. Manson, S., Halford, G. and Hirschberg, M., "Creep-Fatigue Analysis by Strain-range Partitioning," Symposium on Design for Elevated Temperature Environment, ASME, New York, pp. 12-28, 1971.

ACKNOWLEGEMENTS

Special thanks to the following team members David Groebel and Sharon Honecker from Reliasoft Corporation for their support reviewing the results.

BIOGRAPHY

Julio Pulido, PhD
Reliasoft Corporation
Tucson, AZ, USA

e-mail: Julio.pulido@reliasoft.com

Julio Pulido is a Director of Design for Reliability Engineering at Reliasoft Corporation. His responsibility is to drive the capability development of Design for Reliability for consulting clients. He holds BS from the Federal University of Bahia, Brazil, MS from the Federal University of Rio Grande do Sul, Brazil, PhD from Federal University of Rio de Janeiro, Brazil, PhD Research at Duke University and MBA from Xavier University. His specialty is in the area of Structural Analysis, Design for vibration and Structural Reliability, and accelerated testing techniques. He has published over 20 works at different international Symposiums.